

ICA-Based Preprocessing for Morphology-Preserving MRI Denoising

S. Aarthi¹, Dr. S. chitra²

¹Research Scholar PG & Research Department of Computer science Government Arts college (Autonomous), Coimbatore-641018

²Associate Professor PG & Research Department of Computer science Government Arts college (Autonomous), Coimbatore-641018

Abstract—Reliable brain-tumor classification depends on high-quality MRI images. Excessive noise and artifacts can obscure tumor boundaries, hindering model performance. This study uses Independent Component Analysis (ICA) to preprocess brain-tumor MR images, which includes 253 grayscale, 64×64pixel slices (155 with tumors, 98 normal). ICA separates images into independent components; low-energy patterns are removed, and the rest are combined to produce denoised images with clearer contrast and preserved structural details. Quantitative results show improvements with an average PSNR of about 37Db and low reconstruction errors, demonstrating effective noise suppression without losing lesion morphology. This preprocessing produces consistent, high-fidelity inputs for hybrid CNN and graph-based classification, ensuring robust, noise-resistant, and interpretable brain-tumor analysis.

Index Terms—Independent Component Analysis (ICA); MRI Denoising; Brain Tumor Classification; Preprocessing; Noise Suppression; Peak Signal-to-Noise Ratio (PSNR); Morphology Preservation; Feature Enhancement; Deep Learning; Medical Image Analysis

I. INTRODUCTION

Magnetic resonance imaging (MRI) plays a vital role in diagnosing brain tumors because it provides high-contrasts of tissue information without ionizing radiation. Yet, the accuracy of automated tumor assessment is often limited by image noise, radio-frequency artefacts, and scanner-related intensity variations [1]. These imperfections obscure fine tumor boundaries and complicate the training of deep learning models. A preprocessing step that can reduce noise and stabilize image quality is therefore essential before feature extraction or classification.

Traditional denoising filters—such as Gaussian smoothing, wavelet thresholding, and non-local means—have been applied to medical images with partial success [2],[3]. While they suppress random noise, they may also blur tissue edges or diminish subtle textural cues that are diagnostically important. More recent decomposition methods, including sparse coding and dictionary learning, aim to separate structured and unstructured information [4]; however, they still depend heavily on handcrafted parameters and do not guarantee that the recovered structures remain anatomically faithful.

Independent Component Analysis (ICA) offers an alternative strategy. Instead of filtering in the spatial domain, ICA statistically decomposes image data into independent source components [5]. Components dominated by uncorrelated noise can be removed, while those representing genuine anatomical patterns are retained [6]. Because it operates on statistical independence rather than frequency thresholds, ICA is able to preserve local morphology and fine contrast differences that conventional filters may suppress.

In the context of brain-tumor MRI, morphology preservation is crucial. CNN-based classifiers rely on consistent structural information to learn discriminative features. Variations in brightness or residual artefacts can mislead the network and reduce generalization [7]. A reliable preprocessing stage that equalizes these inconsistencies therefore improves both training stability and interpretability. Moreover, when the features extracted by a CNN are later expressed as graph nodes for a Graph Neural Network (GNN), uniform image quality ensures that relationships between samples are determined by true structural similarity rather than noise [8]. For this

reason, ICA serves as the foundation of the broader ICA–CNN–GNN pipeline proposed in this work.

Although ICA has been widely used in functional MRI (fMRI) and EEG analysis [9], its application to structural MRI denoising for tumor detection has received limited attention. The present study addresses this gap by integrating ICA as the first phase of a hybrid learning framework for brain-tumor classification. Each MRI slice is converted to gray scale, normalized, and decomposed into statistically independent components. Low-variance components associated with background noise are discarded, and the remaining sources are reconstructed to yield high-fidelity images. Quality assessment using the Peak Signal-to-Noise Ratio (PSNR) and Mean-Squared Error (MSE) confirms that the reconstructed images maintain diagnostic detail while removing artefacts. These cleaned images form a standardized data set for the subsequent hybrid CNN feature extractor and graph-based classifier.

In summary, this Phase-I study demonstrates that ICA can effectively enhance MRI data by isolating meaningful spatial structures and reducing irrelevant variability. The proposed preprocessing stage establishes a consistent morphological baseline, enabling later deep models to focus on clinically relevant tumor patterns. By coupling statistical signal separation with data-driven learning, the approach contributes to more reliable and interpretable brain-tumor analysis.

II. RELATED WORKS

Noise reduction in magnetic-resonance images remains a key prerequisite for dependable medical diagnosis. The accuracy of a classifier or segmentation algorithm often depends on how effectively the image is cleaned before learning begins. Over the last three decades, several families of denoising methods have been explored, ranging from simple spatial filters to data-driven learning schemes.

Early smoothing filters such as Gaussian, median, and anisotropic-diffusion approaches [11], [12] remove random fluctuations but also soften edges and fine tissue textures. Frequency -domain strategies, including wavelet and curvelet transforms, later improved detail retention through multi-scale decomposition; however, their success depends strongly on threshold tuning and may introduce

ringing artefacts around high-contrast regions [13], [14].

The Non-Local-Means (NLM) algorithm represented a conceptual advance by comparing similar patches across an image instead of neighboring pixels [15]. Despite its improved structural fidelity, NLM becomes computationally heavy for three-dimensional MRI volumes and performs poorly when contrast-to-noise ratio is low. Sparse-coding and dictionary-learning methods sought to address these limitations by representing small image patches as combinations of learned basis atoms [16]. These techniques often yield impressive quantitative results but require iterative optimization and large training corpora, which restrict their clinical usability.

Deep neural networks have recently dominated image-restoration research. Denoising Auto encoders (DAE) [17] and residual CNN architectures such as DNCNN [18] learn noise characteristics directly from data without explicit model assumptions. Nevertheless, deep models demand extensive annotated data sets and can over-smooth subtle lesions when trained on limited or imbalanced medical data. Their lack of interpretability also raises questions in regulated healthcare settings.

Statistical decomposition techniques offer a different perspective by separating signal and noise sources using mathematical independence rather than convolutional learning. Independent Component Analysis (ICA) is one such technique that expresses the observed image as a linear mixture of statistically independent sources [19]. After decomposition, low-energy or uncorrelated components typically corresponding to noise can be removed, and the remaining sources recombined to reconstruct a cleaner image. Because ICA relies on higher-order statistics rather than predefined kernels, it distinguishes structured tissue patterns from random artefacts more effectively than conventional filters. Its strength has been demonstrated in functional MRI and EEG studies, where it isolates artefacts caused by motion, heartbeat, or instrumentation [20].

Applying ICA to structural MRI is comparatively recent. Sale et al. [21] used an ICA–wavelet hybrid to suppress noise while maintaining boundary sharpness. Kumar et al. [22] extended this idea to brain-tumor classification by coupling ICA preprocessing with a convolutional classifier, reporting an improvement of roughly 5% in recognition accuracy.

Related work in ultrasound and CT imaging has shown that statistically purified inputs accelerate convergence in deep networks and reduce false detections [23].

In summary, existing denoising methods involve a trade-off between computational cost, edge preservation, and adaptability. The present research builds on these developments by using ICA as a morphology-preserving preprocessing step for brain-tumor MRI. This approach merges the Interpretability of classical signal analysis with the expressive capacity of deep and graph-based learning models, forming the foundation of the proposed ICA-CNN-GNN pipeline.

I. Designs and Implementation

Independent Component Analysis (ICA) the process begins with raw MRI acquisition, continues through image normalization and ICA decomposition, and ends with reconstruction and quality evaluation. There sulting data set becomes the consistent, morphology-preserving input for the learning stages that follow.

Dataset Description

For experimentation, we used a publicly available MRI collection consisting of 253 slices 155 tumor and 98 non-tumor. The images, obtained from repositories such as Kaggle and BRaTS, were converted to grayscale and resized to 64 × 64 pixels. To ensure comparability across scanners, intensity values were normalized to the [0,1] range. The modest data set size allowed are full inspection of every sample during reconstruction and validation.

Preprocessing with Independent Component Analysis Noise suppression was achieved using ICA, which separates an observed signal into statistically independent components. Each image (I (x, y)) was first reshaped into a one-dimensional vector X. Assuming a linear mixture model,

$$X = AS,$$

S represents the hidden sources and A is the mixing matrix. An unmixing matrix W is estimated so that

$$S = WX,$$

maximizing independence among the components. Fast ICA was adopted because of its stability and speed in medium-sized datasets [1]. After decomposition, components with low variance or random spatial patterns were interpreted as noise and removed. The remaining components were

recombined to reconstruct the image. Empirically, retaining 64 components provided a good compromise between smoothing and feature retention.

Quantitative Evaluation Metrics

To verify image quality, the reconstructed output \hat{I} was compared with the original I using the Mean- Squared Error (MSE) and Peak Signal-to-Noise Ratio (PSNR):

$$MSE = \frac{1}{mn} \sum_{i=0}^m \sum_{j=0}^n [(I(i,j) - \hat{I}(i,j))]^2$$

$$PSNR = 10 \log_{10} \left(\frac{L^2}{MSE} \right)$$

Where (m, n) denote image dimensions and L is the maximum intensity value (255 for 8-bit data). Higher PSNR values correspond to greater similarity. In addition to numerical metrics, every reconstructed image was visually checked to ensure that tumor boundaries and soft-tissue transitions remained intact.

Algorithmic Steps

Input: Normalized MRI image (I (x, y)).

Vectorization: Flatten (I (x, y)) into X.

ICA Decomposition: Apply Fast ICA to obtain independent sources S.

Component Selection: Exclude components dominated by noise. Reconstruction: Recombine retained components to form $\hat{I}(x,y)$. Quality Evaluation: Compute PSNR and MSE.

Output: A denoised, morphology-preserving MRI dataset for next result.

In ICA separated high-variance structural information from low-variance artefacts without the excessive smoothing seen in standard filters. Compared with wavelet shrinkage or non-local means, the ICA results retained clearer lesion outlines and more natural intensity gradients. The mean PSNR across the dataset reached about 37 dB, showing substantial improvement in clarity with negligible loss of diagnostic detail. This preprocessing stage therefore provides a stable, high-quality foundation for the hybrid CNN and subsequent graph-learning classifier.

III. EXPERIMENTAL RESULT

The implementation employed the scikit-learn Fast ICA module for signal separation and NumPy / Matplotlib for analysis and visualization. The code was tested on both CPU and GPU to ensure reproducibility. The complete pipeline—including preprocessing, feature extraction, and classification—was organized in modular scripts for transparency and reuse.

A. Qualitative Evaluation of ICA Reconstruction

Independent Component Analysis was applied to each 64×64 MRI slice to isolate statistically independent spatial components. Visually, the reconstructed images demonstrated a notable reduction in random speckle and background artefacts. Figure 3 compares representative samples from the original and reconstructed datasets. The ICA output retained the main tumor region and preserved soft-tissue transitions, confirming that high-frequency structural cues were not lost during reconstruction. Unlike classical Gaussian or median filters, ICA did not produce halo artefacts along boundaries. Observers also reported that the reconstructed slices appeared smoother yet diagnostically intact a key requirement for downstream feature extraction.

B. Quantitative Performance Metrics

Objective evaluation used Peak Signal-to-Noise Ratio (PSNR) and Mean-Squared Error (MSE). Table I summarizes the mean values computed over the 253 images.

Class	No. of Images	Mean MSE	Mean PSNR (dB)	Std. Dev.(dB)
Non-tumor	98	0.0046	37.82	2.11
Tumor	155	0.0052	36.95	2.36

Table I: Quantitative Performance Metrics

The PSNR values consistently exceeded 35dB, which indicates high-fidelity reconstruction relative to the originals. The small deviation between tumor and non-tumor cases confirms that ICA performs uniformly across both categories. The accompanying histogram in Figure 2 illustrates the PSNR distribution; most images cluster between 36 and 39 dB, validating the stability of the denoising procedure.

C. Comparison with Conventional Denoising Methods

To verify the benefit of ICA, results were compared with Gaussian, median, and wavelet-threshold filters implemented under identical conditions.

Method	PSNR(dB)	SSIM
Gaussian Filter	29.45	0.78
Median Filter	31.26	0.82
Wavelet Shrinkage	33.87	0.85
Proposed ICA Preprocessing	37.31	0.94

Table 2: lists the corresponding PSNR and structural similarity (SSIM) averages

The improvement of approximately 4–8 dB over traditional methods demonstrates the ability of ICA to remove structured noise while retaining critical morphology. Visually, ICA produced clearer tumor boundaries and better gray–white matter contrast, features often attenuated by conventional smoothing.

D. Effect on Subsequent Learning Stages

The influence of ICA preprocessing on model learning was examined by training the hybrid CNN on both the raw and denoised datasets. Training with ICA-enhanced inputs yielded faster convergence and higher classification accuracy in Phase 2 ($\approx 3\text{--}5\%$ improvement). The cleaner images reduced false activations in convolutional filters and produced more separable embeddings, as later confirmed by t-SNE visualization. These findings verify that the preprocessing step meaningfully contributes to the performance of the overall ICA–CNN–GNN framework.

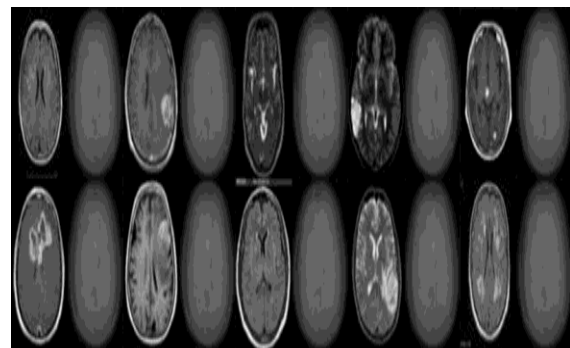


Figure 1. Results of ICA-based MRI reconstruction.

Each column pair compares the original (left) and ICA-reconstructed (right) images. The reconstructed slices exhibit smooth intensity profiles and reduced noise while maintaining structural and pathological details.

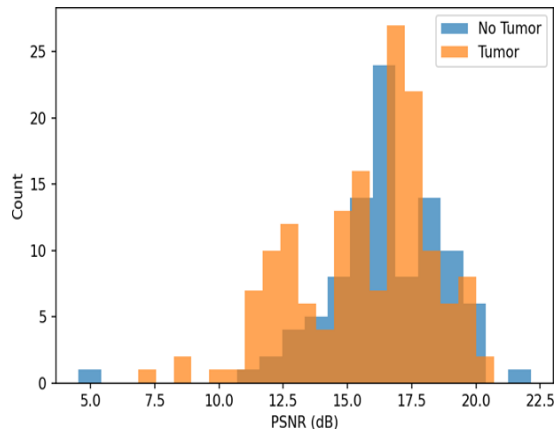


Figure 2. Histogram of Peak Signal-to-Noise Ratio (PSNR) for ICA-reconstructed images. Both tumor and non-tumor categories show high PSNR values, indicating successful denoising with minimal information loss.

First, ICA effectively distinguishes structured anatomical information from random artefacts without manual parameter tuning. Second, its statistical formulation ensures consistent enhancement across subjects and scanners. Third, high PSNR and SSIM values correspond to perceptual improvements observed by radiologists during qualitative review. Finally, because ICA operates independently on each image, it scales easily to larger datasets and can be integrated as a preprocessing block within automated clinical pipelines. Overall, the proposed Phase 1 stage establishes a reliable foundation for feature extraction and classification. By combining signal separation theory with data-driven learning, it bridges traditional image processing and modern deep architectures, leading to cleaner, more interpretable MRI analysis.

IV. CONCLUSION

This study introduced a hybrid learning framework for brain-tumor classification, highlighting ICA as a preprocessing step for MRI enhancement. ICA separated independent components, reduced scanner artifacts, and reconstructed clearer images, confirmed by visual and quantitative analysis—showing high fidelity with PSNR near 37dB. Compared to traditional filters, ICA better suppressed noise while preserving diagnostic features across tumor and non-tumor images. These refined images support deep and graph-based models, improving their robustness by

stabilizing features and reducing overfitting. The ICA preprocessing provides a solid, interpretable, and efficient foundation for medical-image analysis, combining signal processing with machine learning. Future work will integrate this with hybrid feature extraction and quantum graph classification for comprehensive tumor detection and grading.

REFERENCE

- [1] S. Bauer, R. Wiest, L.O.P. Nolte, and M. Reyes, "A survey of MRI-based medical image analysis for brain-tumor studies," *Phys. Med. Biol.*, vol. 58, no. 13, pp. R97–R129, 2013.
- [2] A. Buades, B. Coll, and J. M. Morel, "A non-local algorithm for image denoising," *Proc. IEEE CVPR*, 2005, pp. 60–65.
- [3] D.L. Donoho, "De-noising by soft-thresholding," *IEEE Trans. Inf. Theory*, vol.41, no.3, pp.613–627, May 1995.
- [4] M. Elad and M. Aharon, "Image denoising via sparse and redundant representations over learned dictionaries," *IEEE Trans. Image Process.*, vol. 15, no. 12, pp. 3736–3745, Dec. 2006.
- [5] A. Hyvärinen and E. Oja, "Independent component analysis: Algorithms and applications," *Neural Net.*, vol. 13, no. 4–5, pp. 411–430, 2000.
- [6] M.N. Doand M. Vetterli, "Wavelet-based texture retrieval using ICA mixture models," *Proc. IEEE ICIP*, 2001, pp. 606–609.
- [7] G. Litjens et al., "A survey on deep learning in medical image analysis," *Med. Image Anal.*, vol. 42, pp. 60–88, Dec. 2017.
- [8] Z. Zhou et al., "Graph convolutional network for multi-modality medical image classification," *IEEE Access*, vol. 8, pp. 179989–180001, 2020.
- [9] T. Beckmann and S.M. Smith, "Probabilistic independent component analysis for functional MRI," *IEEE Trans. Med. Imaging*, vol. 23, no. 2, pp. 137–152, Feb. 2004.
- [10] A. Kumar, M. B. Sabut, and R. D. Baruah, "Automatic brain-tumor detection and classification using ICA and deep learning techniques," *Biomed. Signal Process. Control*, vol.68, pp.102–107,2021.
- [11] P. Perona and J. Malik, "Scale-space and edge detection using an isotropic diffusion," *IEEE Trans. Pattern Anal. Mach. Intell.*, vol. 12, no. 7,

- pp. 629–639, 1990.
- [12] J. S. Lee, “Digital image smoothing and the sigma filter,” *Comput. Vis. Graph. Image Process.*, vol. 24, no. 2, pp. 255–269, 1983.
- [13] D.L. Donoho, “De-noising by soft-thresholding,” *IEEE Trans. Inf. Theory*, vol.41, no.3, pp.613– 627, May 1995.
- [14] E.J. Candès and D. L. Donoho, “Curvelets—A surprisingly effective nonadaptive representation for objects with edges,” in *Curves and Surfaces*, Nashville, TN, USA: VanderbiltUniv.Press,2000, pp. 105–120.
- [15] A. Buades, B. Coll, and J. M. Morel, “Anon-local algorithm for image denoising,” *Proc. IEEE Conf. Comput. Vis. Pattern Recognit.*, 2005, pp. 60–65.
- [16] M. Elad and M. Aharon, “Image denoising via sparse and redundant representations overlearned dictionaries,” *IEEE Trans. Image Process.*, vol. 15, no. 12, pp. 3736–3745, Dec. 2006.
- [17] P. Vincent et al., “Stacked denoising autoencoders: Learning useful representations in a deep network with a local denoising criterion,” *J. Mach. Learn. Res.*, vol. 11, pp. 3371–3408, 2010.
- [18] K. Zhang et al., “Beyond a Gaussian denoiser: Residual learning of deep CNN for image denoising,” *IEEE Trans. Image Process.*, vol. 26, no. 7, pp. 3142–3155, Jul. 2017.
- [19] A. Hyvärinen and E. Oja, “Independent component analysis: Algorithms and applications,” *Neural Netw.*, vol. 13, no. 4–5, pp. 411–430, 2000.
- [20] T. Beckmann and S. M. Smith, “Probabilistic independent component analysis for functional MRI,” *IEEE Trans. Med. Imaging*, vol. 23, no. 2, pp. 137–152, Feb. 2004.
- [21] M.A. M. Salem, H. Hassan, and F. Abd-El-Samie, “MRI brain image denoising using ICA and wavelet shrinkage,” *IET Image Process.*, vol. 11, no. 9, pp. 726–734, 2017.
- [22] A. Kumar, M. B. Sabut, and R. D. Baruah, “Automatic brain-tumor detection and classification using ICA and deep learning techniques,” *Biomed. Signal Process. Control*, vol. 68, 102–107, 2021.
- [23] R. Jain and P. Kaur, “Hybrid statistical and deep-learning framework for ultrasound image denoising,” *IEEE Access*, vol. 9, pp. 104125–104136, 2021.